J. Fluid Mech. (1986), *vol.* 166, *pp.* 227–244
Printed in Great Britain

On mixing across an interface in stably stratified fluid

By XUEQUAN E† AND E. J. HOPFINGER
Institut de Mécanique, Université de Grenoble et C.N.R.S., Grenoble, France

(Received 19 March 1985 and in revised form 3 December 1985)

Mixed-layer deepening in stratified fluid has been studied experimentally in mean-shear-free turbulence generated by an oscillating grid. Conditions were varied over a wide range and both two-layered and constant-gradient fluid systems were considered. It is shown that the mixed-layer deepening rate is represented well by power laws, and when local scaling is used all the data can be collapsed on an entrainment relation $E = KRi^{-n}$ with $n = 1.50 \pm 0.05$ when $Ri \gtrsim 7$. This power law suggests that the turbulent kinetic energy is made available for mixing on a buoyancy timescale characteristic of eddy recoil or internal-wave breaking rather than a turbulent-eddy overturning timescale. In the constant-gradient situation internal waves are generated which radiate energy away from the interface. An evaluation of the radiated energy indicates, however, that generally energy radiation does not affect the entrainment rate. The coefficient K therefore has the same value ($K \approx 3.8$) in linearly stratified fluid as in the two-layer situation. The interface thickness is found to be a function of stability, but reaches an asymptotic value of $h/D = 0.055$ when Ri is very large. There is some indication that the interface thickness is also a weak function of Reynolds number.

1. Introduction

Mixing in stably stratified fluids has widespread application in geophysical and environmental fluid systems and has therefore attracted a great deal of interest. This interest is further enlarged by mixing problems related to stratification in industrial situations such as hot-water storage, nuclear-reactor cooling and mixing of different substances in chemical and metallurgical industries.

In the attempt to understand stratification effects, it is attractive to study mixing processes in situations without mean shear, which allows the isolation of phenomena related to turbulence alone. A relatively large number of experiments have therefore considered the situation where turbulence is generated by grid stirring in a stratified fluid layer. Pioneering work on vertical mixing due to turbulence generated by an oscillating grid in a two-layered fluid goes back to Rouse & Dodu (1955) and to Turner (1968), who was the first to propose an empirical relation between the relative entrainment rate E and an overall Richardson number of the form $E \sim \tilde{R}i^{-\frac{3}{2}}$, valid for large Péclet number. This relation has been further supported by the experiments of Hopfinger & Toly (1976) who also related the entrainment rate to a local Richardson number Ri in the form suggested by Turner (1973, p. 291). A mechanistic explanation for the $-\frac{3}{2}$ power law was given by Linden (1973). By projecting vortex rings against an interface, Linden showed that mixing takes place during the recoil

† Permanent address: Institute of Mechanics, Chinese Academy of Sciences, Beijing.

event, which means that the turbulent kinetic energy is made available for mixing at a rate set by the buoyancy timescale. Long's (1978) phenomenological theory assumes that at a high Richardson number the turbulent motions near the interface generate internal waves in the interfacial layer which break intermittently and cause the mixing. Since the response time of these internal waves is again the buoyancy timescale, Linden's and Long's models would seem to be conceptually similar but different in detail. Long's model leads to an entrainment relation $E \sim Ri^{-\frac{7}{4}}$. This relation, although close to $Ri^{-\frac{3}{2}}$, is sufficiently distinct for the difference not to be absorbed by experimental error. Long's model is based on a number of assumptions concerning the mechanism of mixing, and confirmation of the $-\frac{7}{4}$ relation would give strong support to these assumptions.

In two recent papers, Fernando & Long (1983, 1985) give evidence of a close correlation between Long's model predictions and the experimental results. If it is argued that Turner's and Hopfinger & Toly's measurements extend only over about one decade in Ri, the results of Fernando & Long could be accepted to have more general validity. However, Barla (1980) demonstrated a clear $Ri^{-\frac{3}{2}}$ behaviour over at least two decades in Ri.

Chasing power laws of this sort is obviously not very rewarding, and for practical purposes it seems a fruitless task to try to decide between exponents close to each other. Thermocline models, for instance, which are based on energy considerations equivalent to a relation of the form $E \sim Ri^{-1}$, in fairly good agreement with laboratory experiments on convective stirring (Deardorff, Willis & Stockton 1980), give satisfactory prediction of mixed-layer deepening. There is, however, sufficient fundamental incentive to determine the value of the power-law exponent or to give bounds for it, because such experiments set the basis for the development of future models and help to understand the mixing process.

In this paper we present results on mixed-layer deepening in two-layer and linearly stratified fluid, driven by an oscillating grid. The constant density gradient is considered together with the two-layered system in order to see whether radiation of energy by internal waves has any effect. The grid location and grid amplitude and frequency were varied to emphasize the universal character of 'local' scaling. The dependence of interface thickness on local stability, which is a consequence of the mechanism of mixing, is also given. The results presented, although not novel conceptually, clarify a number of questions raised by previous experiments.

2. The experimental conditions

2.1. *The apparatus*

The apparatus used was a revised version of the Hopfinger & Toly (1976) installation. It is a transparent mixing box of 51.4×51.4 cm in cross-section and 70 cm in depth, equipped with a grid of 20 mm square bars, aligned in a square array of mesh $M = 10$ cm. The grid, placed horizontally in the tank, could be oscillated vertically with a stroke $S = 1$–9 cm and with frequencies up to 6 Hz. The important difference with respect to the arrangement used by Hopfinger & Toly lies in the uneven number of meshes to fit into the tank and in the mounting of the grid; the grid was mounted on a 1 cm diameter rod extending throughout the fluid layer. It is thus an upscaled version of Turner's (1968) and McDougall's (1979) arrangement. The advantage is that no fluid is displaced during grid oscillation, and furthermore the grid is easily positioned at any depth in the tank. The uneven number of meshes gives more acceptable wall conditions, that is to say the wall is a plane of symmetry. In the

Hopfinger & Toly experiments the grid had an even number of meshes, with bars sliding near the walls, and this often generated strong motions near the walls. These secondary motions could be kept at an acceptable level only by trial and error, using either an inner box or strips of fine-mesh grids attached to the oscillating grid.

2.2. *Oscillating grid turbulence characteristics*

Turbulence measurements in oscillating-grid turbulence have been made by Thomson & Turner (1975), Hopfinger & Toly (1976), McDougall (1979) and recently by Mory & Hopfinger (1985). All these experiments indicate a spatial decay of the horizontal r.m.s. turbulent velocity u of the form $u \propto z^{-1}$, where z is measured from a virtual origin which, in the present experiments, coincides with the grid midplane. Thomson & Turner's results are indeed also well represented by a z^{-1} power law, as was shown by Hopfinger & Toly. The empirical relation

$$\frac{u}{fs} = CS^{\frac{1}{2}}M^{\frac{1}{2}}z^{-1} \tag{1}$$

proposed by Hopfinger & Toly is a good approximation for the r.m.s. turbulent velocity produced by grids of square bars with $M/d = 5$, oscillated at $f \leqq 6$ Hz (where d is the bar size). The existence of an upper frequency limit has been demonstrated by McDougall. The constant C is close to 0.30 (Hopfinger & Toly).

The growth of the integral lengthscale with distance from the grid is given by

$$l = \beta z. \tag{2}$$

This scale was measured in homogeneous fluid by Thomson & Turner, Hopfinger & Toly and Mory & Hopfinger. The numerical value of β refers to the longitudinal integral lengthscale obtained from the integral of the measured autocorrelation of the horizontal turbulent velocity. If experiments agree on a linear relation of the form (2), they diverge on the actual value of β. Hopfinger & Toly found a dependence of β on stroke S when $S/M \leqq 0.8$, whereas recent measurements by Mory & Hopfinger (1985) indicated that β at $S/M = 0.8$ is little different from the value $\beta = 0.10$ at $S/M = 0.2$ (Thomson & Turner 1975). The autocorrelations in the Mory & Hopfinger experiments had however a large negative part, leading to a smaller value of the integral scale. As will be seen later (§4), the actual value of β is of importance for the determination of the proportionality coefficient in the entrainment relation. In the analysis of the results we use $\beta = 0.10$ when $S/M = 0.2$, and for the larger values of S/M, β is chosen such as to make the experiments with $S/M = 0.2$ and 0.85 collapse on one curve, but the same values of β are then used in the two-layered and constant-density-gradient fluids.

Oscillating-grid turbulence, like ordinary grid turbulence, is sensitive to initial conditions. Besides the requirement of sufficiently low solidity $\leqq 0.45\,\%$, the decay depends on the initial energy distribution. An initial excess of energy at large scales gives rise to a more rapid decay of energy than an initial energy deficiency at large scales. Oscillating grid turbulence is, in addition, strongly affected by the grid geometry near the wall. Experiments show that an end condition that considers the wall as a plane of symmetry is the best choice for obtaining a homogeneous turbulent field. The gap between the wall and the ends of the grid bars must be kept as small as possible.

2.3. *Configurations studied*

In all experiments, the total fluid column was 60 cm in depth. The density (salinity) stratification of the fluid column shown schematically in figure 1 was either

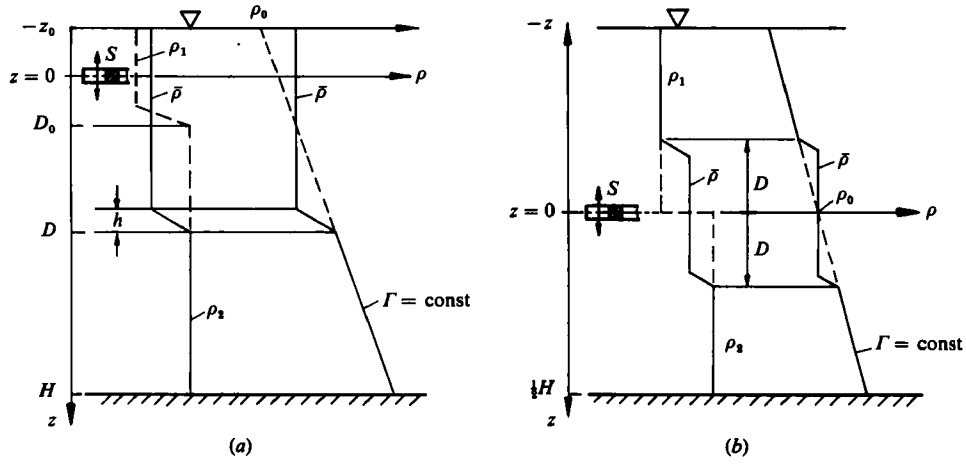

FIGURE 1. Schematic diagram of the experimental arrangements.

two-layered, with the interface 22 cm below the free surface in configuration of figure 1(*a*), or consisted of a constant density gradient. Some experiments were conducted with a constant-density-gradient layer adjacent to an interface or to a homogeneous layer to study the importance of the wave-energy flux (see §6).

The grid was positioned either near the top, 11 cm below the free surface, or in the centre of the fluid column (figure 1*b*). When in the top position the stroke was set at 8.5 cm with frequency 1–3 Hz. In the centre position only a 2 cm stroke was used, with frequency up to 6 Hz. Exceptions to this were some experiments emphasizing internal-wave-energy radiation, reported in §6.

The depth of the mixed layer was determined from shadowgraph records to an accuracy of ± 0.2 cm. Conductivity-probe traverses along the vertical were made to determine the interface thickness.

To visualize wave motions in the constant-gradient region, 200 μm diameter wood particles were introduced in the fluid, and a vertical slice of fluid was illuminated. The density of wood particles depends on the time of immersion in water. After about 20 min their density is close to 1.00 g/cm^3. The maximum density is 1.17 g/cm^3.

3. Mixed-layer deepening in time

3.1. *Grid position near the top*

Taking the z'axis as positive-downward with $z' = z+z_0$ (figure 1*a*), the density $\rho(z)$ is given by

$$\rho = \begin{cases} \bar{\rho} & (-z_0 < z < D-h), \\ \rho_2 & (D < z < H) \end{cases} \tag{3}$$

for the two-layer stratification, and by

$$\rho = \begin{cases} \bar{\rho} & (-z_0 < z < D-h), \\ \rho_0 + \Gamma z' & (D < z < H) \end{cases} \tag{4}$$

for the constant-density-gradient Γ fluid. The interface thickness h is generally small compared with D. When the interface thickness is supposed constant, the expression

for $\bar{\rho}$ and the density jump $\Delta\rho$ across the interfacial layer are for system (3) given by

$$\bar{\rho} = \rho_1 \frac{z_0+D_0}{z_0+D} + \rho_2 \frac{D-D_0}{z_0+D}, \quad \Delta\rho = (\rho_2-\rho_1)\frac{z_0+D_0}{z_0+D}, \tag{5a, b}$$

where D_0 is the initial position of the interface measured from the mid position of the grid and ρ_1 and ρ_2 are the initial densities of the upper and lower layers respectively (see figure 1). The linear stratification expressed by (4) gives

$$\bar{\rho} = \frac{\Gamma}{2}(D+z_0)\left[1-\frac{h}{2(D+z_0-h)}\right]+\rho_0, \quad \Delta\rho = \frac{\Gamma(D+z_0)^2}{2(D+z_0)-h}. \tag{6a, b}$$

To establish a relation for the mixed-layer deepening rate, an assumption must be made on the conversion of kinetic-energy flux into the interface and the rate of change of potential energy. The assumption of proportionality used by Linden (1975) leads to the relations $D \propto t^{\frac{1}{2}}$ for the two-layered fluid and $D \propto t^{\frac{1}{3}}$ for a constant-gradient fluid.

Long's model gives respectively for stratifications (3) and (4)

$$D \propto \left(g\frac{\Delta\rho_0}{\rho_2}d_0\right)^{-\frac{1}{11}}(fS)^{\frac{5}{11}}(SM)^{\frac{3}{11}}t^{\frac{4}{11}} \quad (D \gg z_0, D_0), \tag{7}$$

where
$$d_0 = D_0 + z_0,$$

and
$$D \propto N^{-\frac{2}{15}}(fS)^{\frac{1}{3}}(SM)^{\frac{1}{5}}t^{\frac{4}{5}}, \tag{8}$$

where
$$N^2 = \frac{g}{\rho_0}\frac{\partial\rho}{\partial z} = \frac{g\Gamma}{\rho_0}.$$

The power laws (7) and (8) together with (1) and (2) are consistent with an entrainment relation $E \propto Ri^{-\frac{1}{2}}$. On the other hand, the time dependence of mixed-layer deepening consistent with (1) and (2) and

$$E \equiv \frac{u_e}{u} = KRi^{-\frac{1}{2}}, \tag{9}$$

where $u_e = \mathrm{d}D/\mathrm{d}t$ and $Ri = g(\Delta\rho/\bar{\rho})\,l/u^2$, are for the two-layer stratification

$$D \propto \begin{cases} \left(g\dfrac{\Delta\rho_0}{\rho_2}d_0\right)^{-\frac{1}{10}}(fS)^{\frac{1}{2}}(SM)^{\frac{1}{5}}t^{\frac{4}{5}} & (D \gg z_0, D_0), \\ t^{\frac{1}{3}} & (D \ll z_0, D_0 = 0), \end{cases} \tag{10}$$

and for the constant-gradient situation

$$D \propto \begin{cases} N^{-\frac{1}{2}}(fS)^{\frac{1}{2}}(SM)^{\frac{1}{4}}t^{\frac{1}{2}} & (D \gg z_0), \\ t^{\frac{1}{3}} & (D \ll z_0). \end{cases} \tag{11}$$

Expression (9) has support from experiments by Turner (1968, 1973) and Hopfinger & Toly (1976) and can be explained by Linden's (1973) mixing model.

3.2. *Grid positioned in the centre*

Positioning the grid in the centre simplifies the expressions for $\bar{\rho}$ and $\Delta\rho$ and has the advantage that $z_0 = 0$. For the two-layer stratification $\bar{\rho} = \frac{1}{2}(\rho_1+\rho_2)$ and

$\Delta\rho = \frac{1}{2}(\rho_2 - \rho_1)$ and for the constant-gradient situation $\bar{\rho} = \rho_0$ and $\Delta\rho = \Gamma D$. The power laws corresponding to $E \sim Ri^{-\frac{3}{2}}$ are

$$D \propto \left(g\frac{\Delta\rho_0}{\rho_0}\right)^{-\frac{3}{13}} (fS)^{\frac{8}{13}} (SM)^{\frac{4}{13}} t^{\frac{8}{13}}, \tag{12}$$

$$D \propto N^{-\frac{3}{8}} (fS)^{\frac{1}{2}} (SM)^{\frac{1}{4}} t^{\frac{1}{8}} \tag{13}$$

respectively for the two-layer fluid and the constant-density-gradient fluid.

3.3. *Experimental results*

Depth–time relations

In figures 2 (*a*, *b*) the experimental depth–time relations are plotted on a logarithmic scale for the two-layer stratification. Figure 2 (*a*) is for stirring near the top with $S = 8.5$ cm, and figure 2 (*b*) refers to the arrangement shown in figure 1 (*b*) with $S = 2$ cm. It is seen from these figures that the power laws $D \propto t^{\frac{1}{2}}$, (10), and $D \propto t^{\frac{8}{13}}$, (12), are very good representations of the data. Least-square fits to six runs carried out in the situation of figure 2 (*a*) give a slope of 0.195 ± 0.01, and for the arrangement of figure 2 (*b*) the slopes of six runs lie within 0.156 ± 0.002. The correlation coefficient was always 99 % or more.

It can be argued that (10) is valid only when $D \gg z_0$, which is clearly not entirely satisfied by the experimental conditions corresponding to figure 1 (*a*). An effect related with z_0 and D_0 would tend to decrease the exponent of t at small values of D. Figure 1 (*a*) indicates that at large values of D the slope tends to decrease rather than increase. When the grid is located in the centre of the fluid these difficulties are eliminated. Figure 2 (*b*) clearly indicates good agreement of the experiments with the suggested power law $D \propto t^{\frac{8}{13}}$, (12).

The results obtained for the time dependence of the mixed layer in a constant-gradient fluid are also in excellent agreement with (11) and (13). This is shown in figures 3 (*a*, *b*), where D is plotted on a logarithmic scale as a function of time. Least-square fits to six sets of data gave a slope of 0.129 ± 0.005 for the conditions of figure 3 (*a*), and 0.125 ± 0.010 for the conditions of figure 3 (*b*), for which eight experimental runs were performed. Again, the results in figure 3 (*a*), which where obtained by stirring near the top, are subject to errors resulting from a finite value of z_0. The good agreement between the results presented in figures 3 (*a*) and (*b*) indicates, however, that this error remains negligible.

Frequency dependence

The frequency dependence is a further check on the consistency of the results. From figures 2 and 3 we can determine the coefficients $K_i (i = 1$ for the two-layer case and $i = 2$ for the constant-gradient fluid) in

$$D = K_i t^{n_i}$$

and then determine the exponent of the frequency from $K_i = C_i f^{\alpha_i}$ by a least-square fit of K_i versus f. The values for K_i, C_i, n_i and α_i are given in table 1. In general, good agreement is obtained between the predicted and measured frequency dependence. The higher exponent of f in the case where the grid was positioned in the centre of the fluid column is due to the fact that the stratification was not quite the same at the three frequencies (see table 1). No correction was applied to the values K_1 and K_2, which would account for the lower values of $\Delta\rho_0/\rho_2$ and N at the higher frequencies. Since K_i increases when, for the same frequency, the stratification is decreased, the exponent of f is somewhat overestimated.

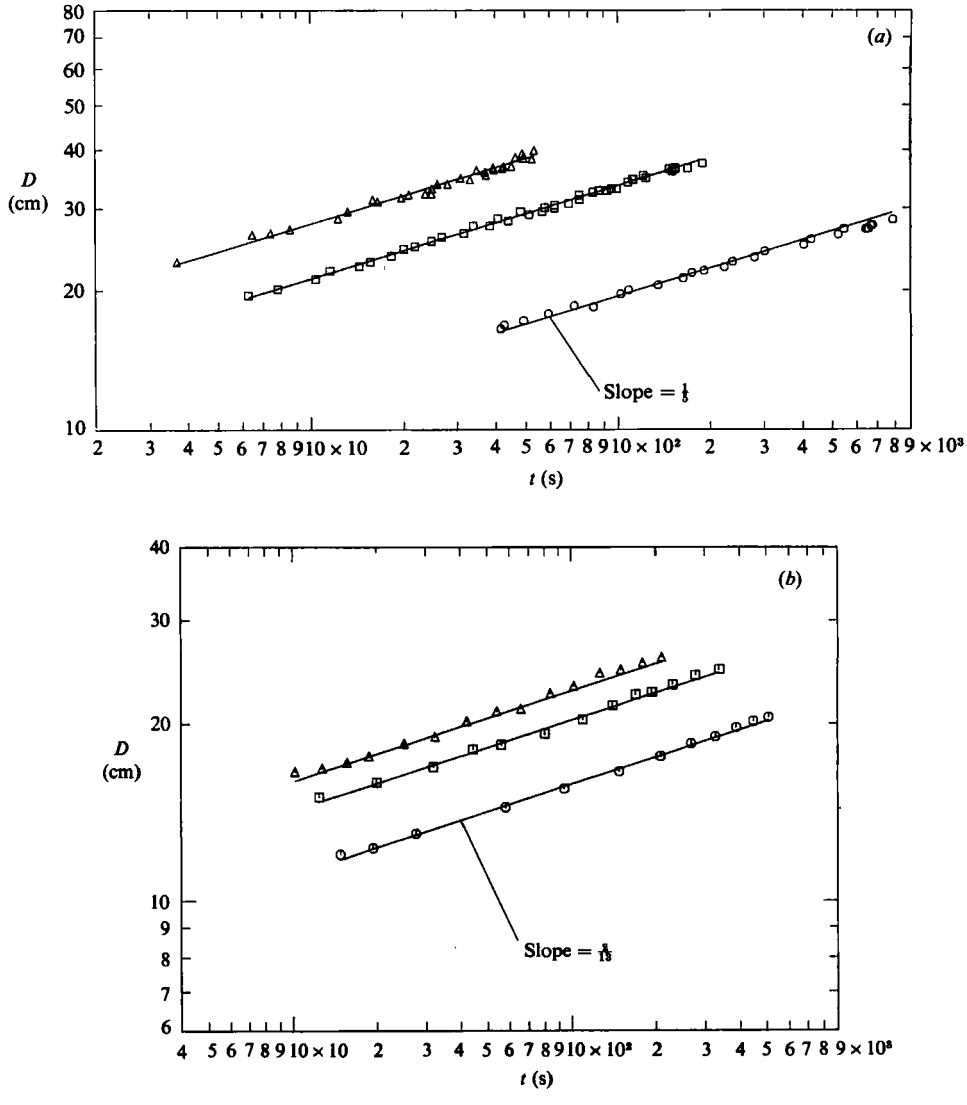

FIGURE 2. Mixed-layer depth D, measured from the grid midplane, plotted logarithmically as a function of time for two-layer fluid. (*a*) Grid positioned near the top (figure 1*a*), oscillated with stroke $S = 8.5$ cm and a frequency $f = 1$ Hz (○), 2 Hz (□), 3 Hz (△); initial stratification $\Delta\rho_0/\rho_2 = 4.75\%$ with $D_0 = 11$ cm. (*b*) Grid positioned in the centre (figure 1*b*) with $S = 2$ cm: ⊙, $f = 4$ Hz, $\Delta\rho_0/\rho_2 = 3.65\%$; ⊡, 5 Hz, 3.38%; ⧋, 6 Hz, 2.90%. In (*a*) and (*b*) the solid lines indicate the power laws (10) and (12).

4. Entrainment relation and mechanism

4.1. *Richardson-number dependence*

The results on mixed-layer deepening presented in §3 are consistent with an entrainment relation given by (9), when it is assumed that the variations with depth of the r.m.s. turbulent velocity and the integral scale follow relations of the form (1) and (2). In homogeneous fluid a dependence of $u \propto z^{-1}$ corresponds to a time variation $D \propto t^{\frac{1}{2}}$. This $\frac{1}{2}$ power variation of the turbulent layer depth has again been verified for the present conditions.

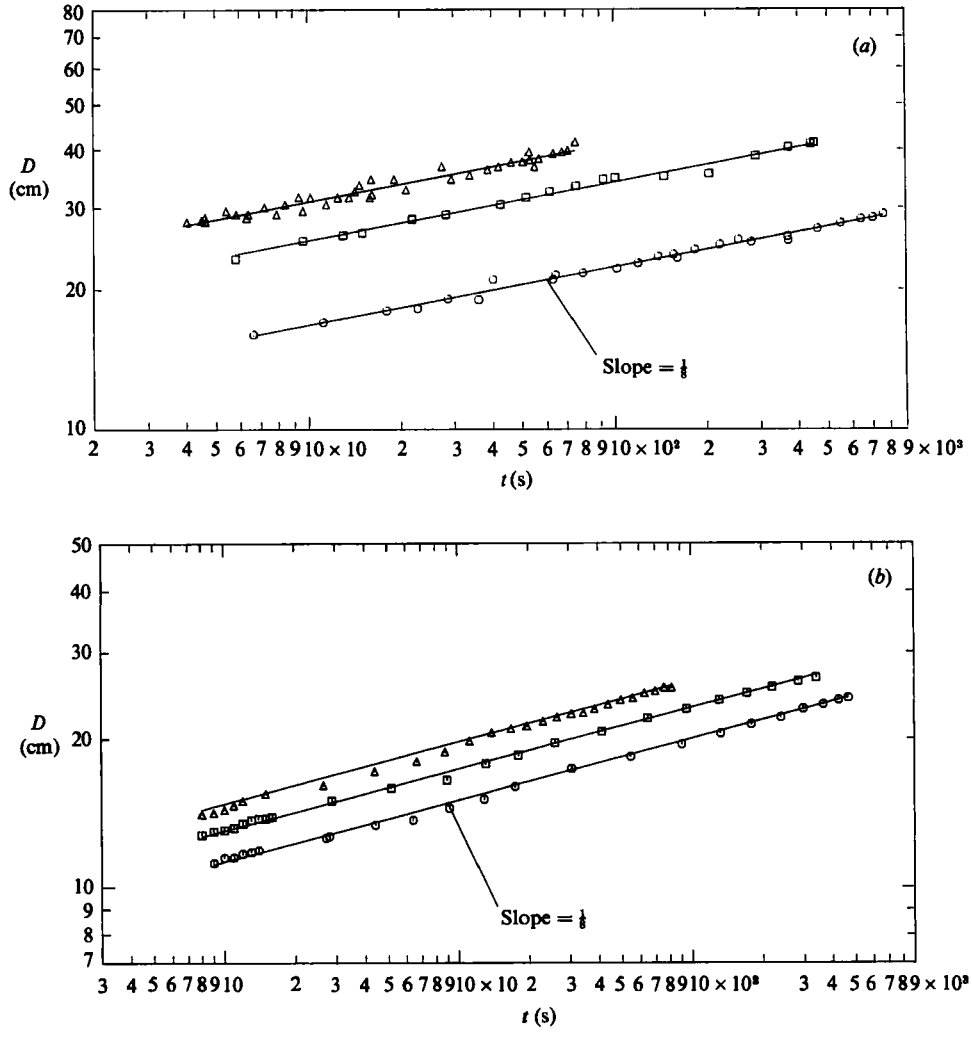

FIGURE 3. Mixed-layer depth versus time in linearly stratified fluid. (*a*) Grid near the top with $S = 8.5$ cm and $f = 1$ Hz, $N = 1.278$ s^{-1} (○), 2 Hz, 1.227 s^{-1} (□) 3 Hz, 1.195 s^{-1} (△). (*b*) Grid in centre with $S = 2$ cm and $f = 4$ Hz, $N = 1.189$ s^{-1} (Ⓣ), 5 Hz, 0.75 s^{-1} (▣), 6 Hz, 0.693 s^{-1} (⚠); ——, power laws (11) and (13).

Since (9) relates the entrainment velocity to local turbulence quantities, all the experiments should be representable by the same unique relation. Figures 4(*a*) and (*b*) show logarithmic plots of the entrainment coefficient $E = u_e/u$ as a function of local Richardson number $Ri = g\Delta\rho l/\bar{\rho}u^2$ for the two-layer fluid and the constant-gradient layer respectively. For the sake of clarity two separate graphs are given. The entrainment velocity u_e was determined from the measured rates of deepening of the mixed layer, and u and l used in the expression for the Richardson number were calculated from (1) and (2), with $z = D$. The value of β in (2) was taken equal to 0.10 when $S = 2$ cm. With stroke $S = 8.5$ cm the value of β necessary to make the data, obtained with $S = 2$ cm, collapse with those of 8.5 cm for the two-layer stratification (figure 4*a*) is $\beta = 0.24$. The best collapse for the linearly stratified situation is

	S (cm)	f (Hz)	$\Delta\rho_0/\rho_2$ (%)	K_1 (cm s^{-n_1})	n_1	C_1 (cm $s^{\alpha_1-n_1}$)	α_1
			Two-layered				
Grid near top	8.5	1	4.75	4.87	$\frac{1}{5}$	4.9	—
		2		8.43			0.75
		3		11.06			(0.8)
Grid in central position	2	4	3.65	5.45	$\frac{2}{13}$	2.05	—
		5	3.38	6.99			0.75
		6	2.90	7.85			(0.62)
	S (cm)	f (Hz)	N (s^{-1})	K_2 (cm s^{-n_2})	n_2	C_2 (cm $s^{\alpha_2-n_2}$)	α_2
			Constant-gradient				
Grid near top	8.5	1	1.2787	9.43	$\frac{1}{8}$	9.51	—
		2	1.2270	14.35			0.50
		3	1.1956	17.37			(0.50)
Grid in central position	2	4	1.189	8.45	$\frac{1}{8}$	3.21	—
		5	0.705	9.77			0.64
		6	0.693	11.09			(0.50)

TABLE 1. Numerical values for the depth–time relation $D = C_i f^{\alpha_i} t^{n_i}$ ($i = 1$, two-layered fluid; $i = 2$, constant-gradient). The values of α_i in parentheses are the theoretical values.

obtained with $\beta = 0.23$. This value of β is well within the variations of β suggested by Hopfinger & Toly. All the results collapse on a relation

$$E = KRi^{-n}, \quad \text{with } n = 1.54 \pm 0.05.$$

The individual data sets show larger dispersions, and least-square fits to the experimental points obtained in the two-layered fluid resulted in $n = 1.45 \pm 0.05$ for the experiments with $S = 8.5$ cm and 1.40 ± 0.15 when $S = 2$ cm with the grid in the centre. The linearly stratified fluid results gave slightly higher slopes: $n = 1.5 \pm 0.08$ when $S = 8.5$ cm, and $n = 1.50 \pm 0.15$ when $S = 2$ cm. These results substantiate the earlier findings of Turner (1968) and Hopfinger & Toly (1976).

The proportionality coefficient K is also of interest. For both the two-layer and constant-gradient fluids we get from figures 4 (a, b) a value $K \approx 3.8$† comparable to $K \simeq 2.5$ indicated by the results of Turner (see Turner 1973, p. 291) and Hopfinger & Toly. The somewhat higher value of K in the present experiments is due to a slight underestimation of u by using $C = 0.3$ in (1). The value of K is very sensitive to errors in u and should not be given undue emphasis. It may be noted, however, that Fernando & Long's (1985) data give a much larger value of K. When using $C = 0.3$ for the correlation of their data we find $K \simeq 22$. This rather high value of K would indicate that the turbulent velocity was larger by a factor of about 1.5 than would be predicted by (1) with $C = 0.3$. Strong secondary motions generated by the end conditions of the grid in their experiments may have been the cause of this rather high effective turbulent velocity. In the presence of strong secondary motions the spatial decay rate is likely to be different near the grid than further away from it. The experiments of Hopfinger & Toly (1976) give some indication of such different decay rates.

† $\simeq$ means roughly equal to within an uncertainty factor of 0.8–1.2; $\approx$ 0.6–1.8; $\sim$, $\frac{1}{3}$–3.

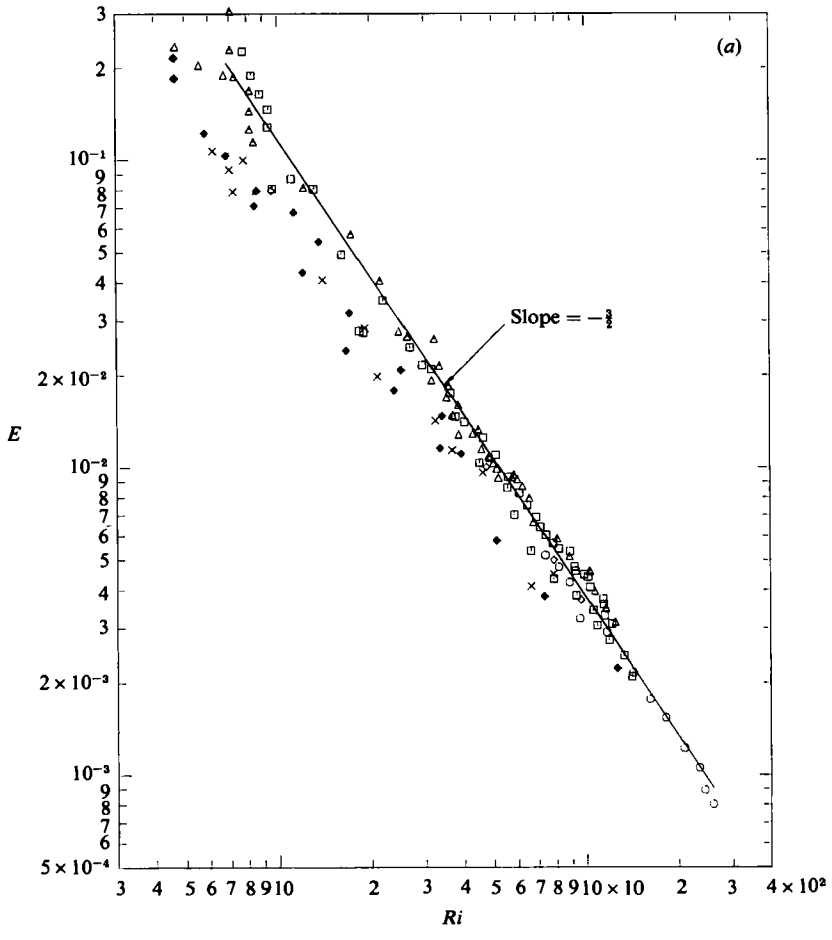

FIGURE 4(*a*). For caption see facing page.

The power-law correlation is valid only beyond a certain value of Richardson number. When Ri is small a turbulent eddy entering the interfacial layer will tend to thicken the interface, whereas when Ri is large the interface will remain sharp. This aspect has been discussed by Linden (1979) by evaluating the flux Richardson number as a function of overall stability for different stratified-flow experiments. In oscillating-grid experiments the change occurs at a Richardson number $Ri \approx 7$, as can be seen from figures 4(*a*, *b*). This behaviour can also be interpreted in terms of collapse of turbulence in stratified fluid which is characterized by a local Foude number $u/Nl \approx 0.3$ (Dickey & Mellor 1980; Browand & Hopfinger 1985) here related to the local interfacial Richardson number by $Ri = (1/0.3)^2 h/l$, where h is the interface thickness. Since in general in the experiments h is of order l (see §5), the local Froude number criterion gives a reasonable indication of the change in the E versus Ri relation. The experimental scatter is unfortunately too large to determine any influence of h/l.

4.2. *Entrainment mechanisms*

The present paper emphasizes questions concerning the entrainment relation, the interface thickness and possible effects of energy radiation by internal waves. The

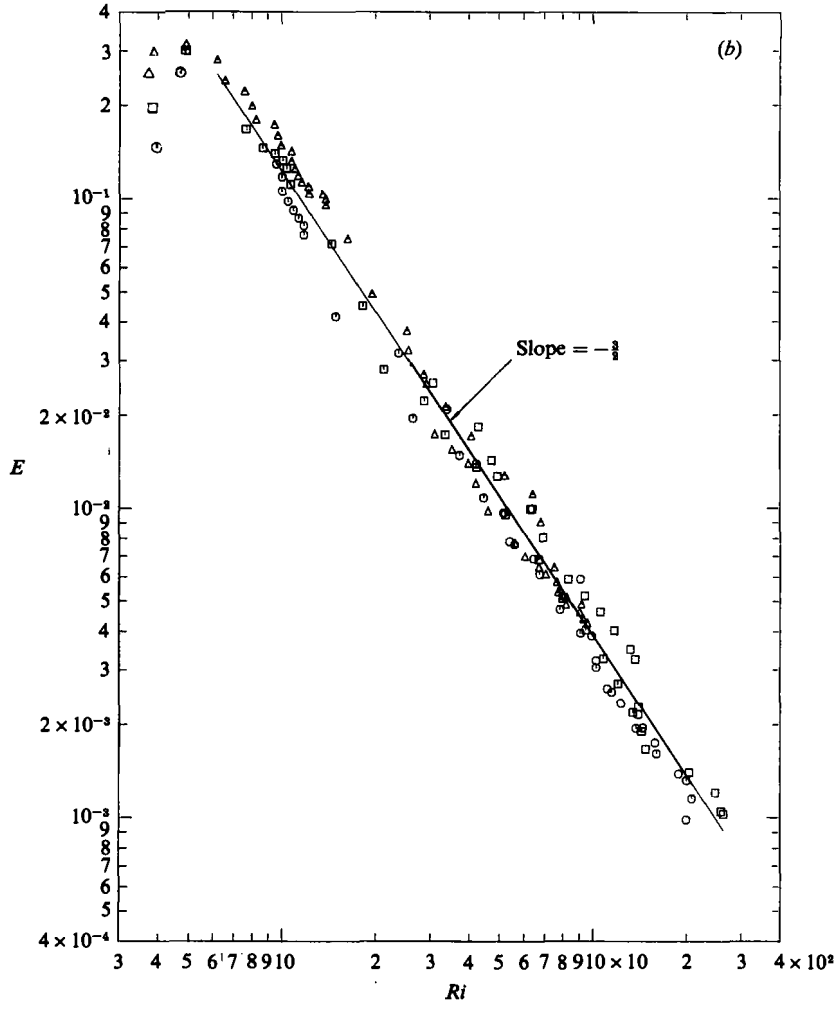

FIGURE 4. Entrainment rate $E = u_e/u$ plotted logarithmically as a function of local Richardson number $Ri = g\Delta\rho l/\bar{\rho}u^2$. (*a*) Two-layer fluid: ○, $f = 1$ Hz, $S = 8.5$ cm; □, 2 Hz, 8.5 cm; △, 3 Hz, 8.5 cm; ⊡, 5 Hz, 2 cm; ⧋, 6 Hz, 2 cm. For comparison, Turner's (1973) data (◆) and Hopfinger & Toly's data (×) are included. The slope $-\frac{3}{2}$ is the best fit to the present data. (*b*) Constant-density-gradient fluid: ○, $f = 1$ Hz, $S = 8.5$ cm; □, 2 Hz, 8.5 cm; △, 3 Hz, 8.5 cm; ⊙, 4 Hz, 2 cm, ⊡, 5 Hz, 2 cm; ⧋, 6 Hz, 2 cm; ——, slope $-\frac{3}{2}$. In both cases u and l were calculated from (1) and (2) with $z = D$.

entrainment mechanism would need a separate, more sophisticated investigation. However, since the questions addressed are intimately related to the entrainment mechanism, it seems valuable to give it some consideration.

When the Richardson number is low ($Ri \sim 1$), entrainment is by engulfment, just as in non-stratified fluids. The turbulent–non-turbulent interface has large excursions. As the Richardson number increases, the interface smoothes out, and when Ri is large, the perturbations at the boundary between the interfacial layer and the non-turbulent fluid become very small. This change with stability of the interfacial layer structure is shown in figures 5(*a–c*), which are shadowgraphs taken at $Ri = 22.1(a)$, $53.9(b)$ and $199.8(c)$. These photographs also show an increasing number of striations in the interfacial layer (figure 5*c*) with increasing Ri, which is

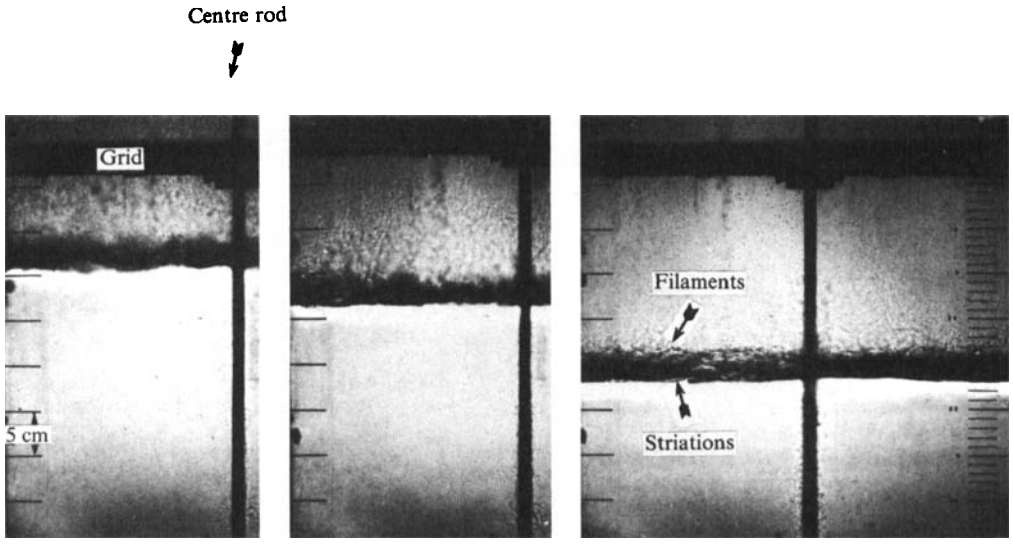

FIGURE 5. Shadowgraphs showing the mixed-layer deepening (from grid to interface) and the change in interfacial-layer structure. The layer below is stably stratified with $N = 1.278\ \mathrm{s}^{-1}$. The grid is oscillated with frequency $f = 1$ Hz and with stroke $S = 8.5$ cm. (*a*) 33 s after starting grid, $D = 14$ cm, $Ri = 22.1$; (*b*), 227 s, $D = 18$ cm, $Ri = 53.9$; (*c*), 3625 s, $D = 27$ cm, $Ri = 199.8$.

indicative of strong density gradients caused by internal-wave motions. These strong gradients enhance the mass flux through the interfacial layer from its non-turbulent edge to the turbulent boundary, where wisps or filaments of fluid are then lifted off and mixed through the turbulent layer. These ejections of fluid into the turbulent layer may be a result of eddy recoil, as was suggested by Linden (1973) and of internal-wave breaking as suggested by Long (1978).

Linden's recoil mixing model is based on the observations he made in his vortex ring experiment (Linden 1973) that the turbulent kinetic energy is not made available for mixing with the incoming turbulent velocity u, but rather with a recoil buoyancy velocity d/τ_B, where d is the penetration depth of the eddies, $d \sim \bar{\rho}u^2/g\Delta\rho$, and $\tau_B \sim (\bar{\rho}l/g\Delta\rho)^{\frac{1}{2}}$ is the response time of the interfacial layer to disturbances of lengthscale l. The relation

$$\frac{\bar{\rho}u^2 d}{\tau_B} \sim D\frac{\mathrm{d}D}{\mathrm{d}t}g\Delta\rho$$

then gives $u_e/u \sim Ri^{-\frac{3}{4}}$. This very simple model seems to contain the essential physics. It is important to note that internal-wave breaking has a similar scaling. In a footnote Linden points out that the ejections caused by breaking internal waves of length $\lambda \sim l$ also have a timescale $(\rho l/g\Delta\rho)^{\frac{1}{2}}$, and thus make the kinetic energy available for mixing at a similar rate as the recoil mechanism. It is our belief that Long's model has a valid physical basis, but the detailed steps leading to the $Ri^{-\frac{3}{4}}$ relation may incorporate some assumptions not supported by experiments.

5. Interfacial-layer thickness

The interface thickness is a signature of the mechanisms of mixing across an interface. As was mentioned above, when the stratification is weak or moderate, local instabilities can occur which thicken the interface. With strong stratification, mixing

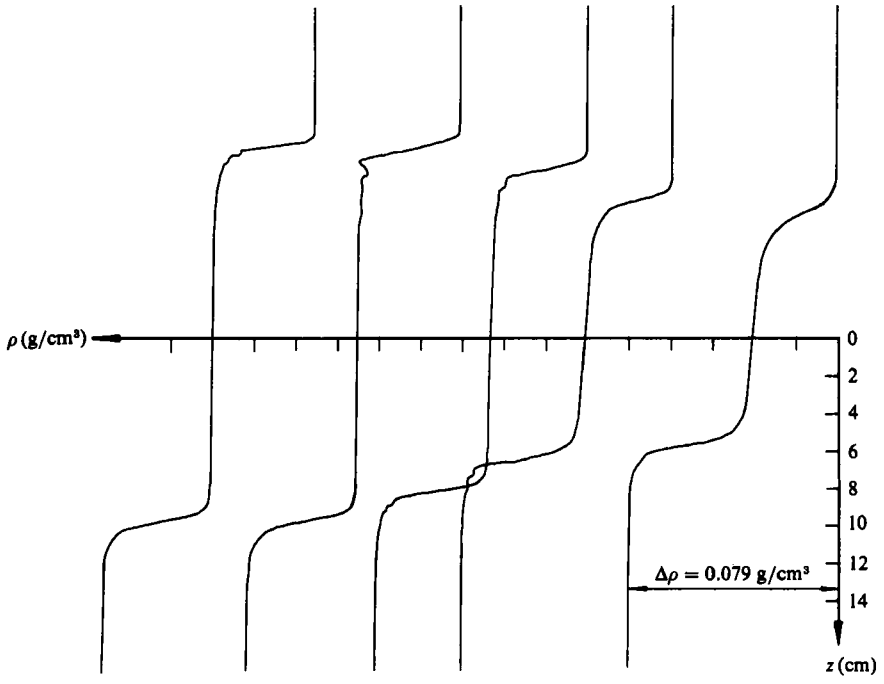

FIGURE 6. Recordings of density variations from conductivity-probe output with grid in central position in two-layer fluid ($f = 5$ Hz, $S = 2$ cm).

may be caused by the lift off of filaments due to intermittent breaking of (resonant) internal waves as suggested by Long (1978) or due to the recoil of impinging eddies (Linden 1973). The interface thickness should therefore depend on stability conditions, at least in the moderately high-Richardson-number range. Results obtained for penetrative convection experiments by Deardorff *et al.* (1980) suggest that the interface thickness, normalized by the mixed-layer depth, is a decreasing function of Ri, with an asymptotic value at high values of Ri. For grid-stirring experiments Fernando & Long (1985) concluded that h/D is nearly independent of Ri.

In the present experiments the interface thickness was determined from $h = (\mathrm{d}\rho/\mathrm{d}z)_{\max}/\Delta\rho$. This definition corresponds to Crapper & Linden's (1974) definition and to h_2 of Fernando & Long (1985). The density gradient was obtained from recordings of the mean of the output of three conductivity probes dropped simultaneously through the fluid layer. A typical example of such recordings is shown in figure 6, with the grid in the centre of the fluid column.

In figure 7 we have plotted the interface thickness normalized by D as a function of Ri for linearly stratified fluid, with the grid oscillated at different frequencies and with stroke $S = 2$ cm. This figure indicates a clear dependence of h/D on Ri, with h/D varying from 0.15 for low values of Ri (≈ 10) to 0.06 when Ri is large (≈ 200). A good functional representation is

$$h/D = 0.055 + 0.91\, Ri^{-1}.$$

The behaviour of h/D for conditions $S = 8.5$ cm, shown in figure 8, can also be approximated by this relation. There is, however, a tendency for the asymptotic

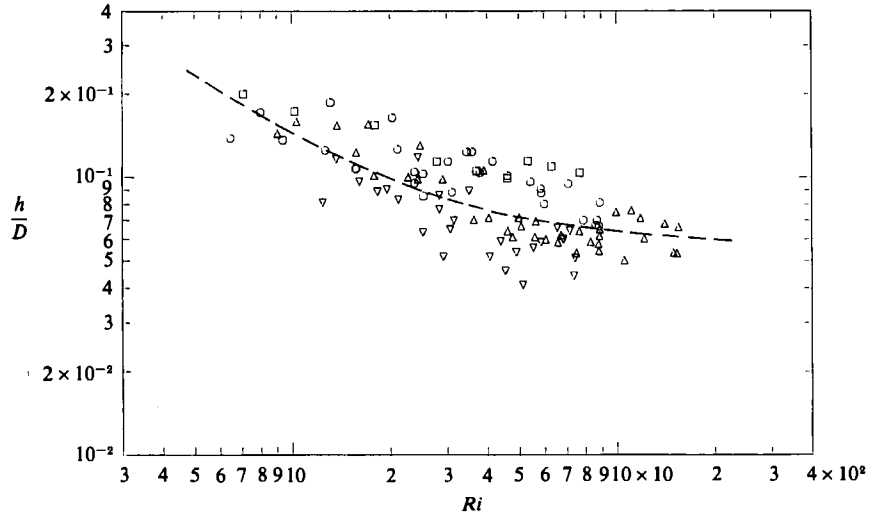

FIGURE 7. Non-dimensionalized interface thickness h/D plotted as a function of Ri for linearly stratified fluid with grid in central position, oscillated with $S = 2$ cm and $f = 2$ Hz, $N = 0.599$ s^{-1} (○), 4 Hz, 0.613 s^{-1} (□), 5 Hz, 0.652 s^{-1} (△), 6 Hz, 0.664 s^{-1} (▽); --- is $h/D = 0.055 + 0.91\ Ri^{-1}$.

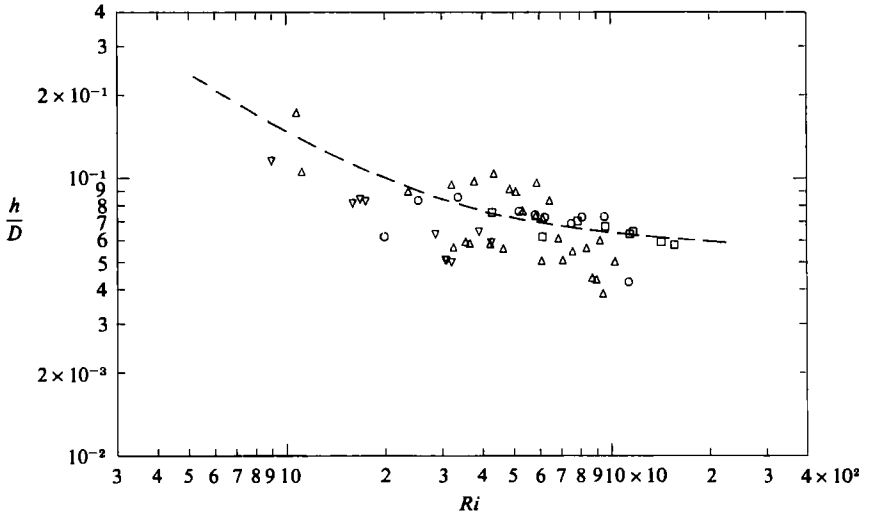

FIGURE 8. Non-dimensionalized interface thickness h/D as a function of Ri for linearly stratified and two-layer fluid with grid positioned near top, oscillated with $S = 8.5$ cm and $f = 2$ Hz, $N = 1.250$ s^{-1} (○), $f = 1$ Hz, $\Delta\rho_0/\rho_2 = 4.75\%$ (□), 2 Hz, 4.75% (△), 3 Hz, 4.75% (▽); ---- is $0.055 + 0.91\ Ri^{-1}$.

value of h/D to be lower when $S = 8.5$ cm, which would seem to exclude a scaling of h on l.

The considerable scatter in figures 7 and 8 cannot solely be attributed to experimental uncertainty. There is some fairly consistent trend for h/D to be smaller when, for constant Ri, the grid oscillation frequency is increased. This might be indicative of some Reynolds-number dependence at intermediate values of Ri.

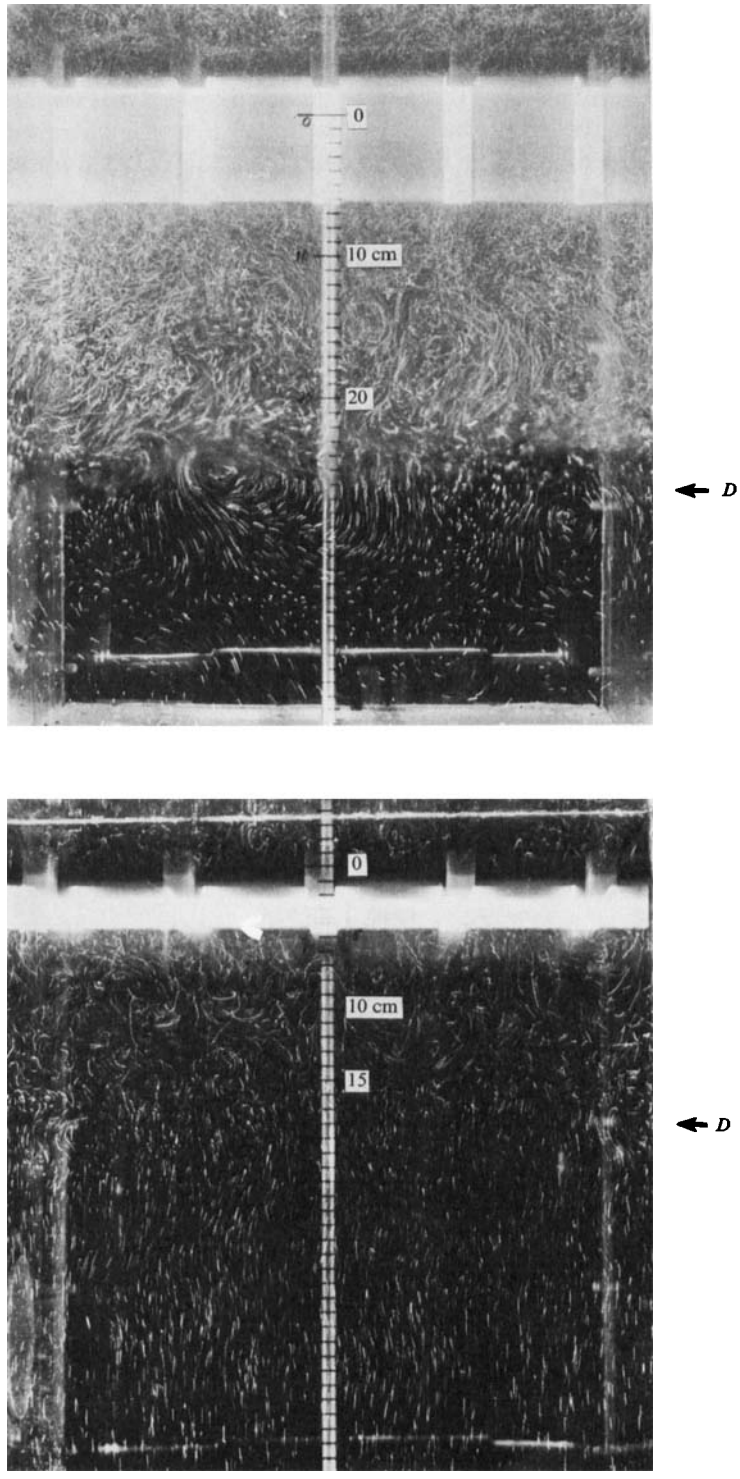

(*a*)

(*b*)

FIGURE 9. Streakline photograph showing internal-wave motion in the constant gradient layer below the interface. (*a*) Conditions are $S = 8.5$ cm, $f = 3$ Hz, $N = 1.251$ s^{-1}, $D = 26.6$ cm, $\Delta\rho/\bar{\rho} = 0.030$, $Ri = 26$, $h \simeq 2$ cm; the exposure time is 1 s. (*b*) $S = 2$ cm, $f = 2$ Hz, $N = 1.12$ s^{-1}, $D = 17$ cm, $\Delta\rho_0/\rho_1 = 0$, $Nl/u = 5$; the exposure time is 4 s. In the stably stratified layer the particles have a free-fall velocity $\simeq 0.5$ cm s^{-1} in (*b*).

6. Energy radiation by internal waves

In the present experiments the entrainment rate of the constant-gradient fluid was in no measurable way affected by energy radiation by internal waves. This is deduced from the fact that the proportionality coefficient K in the entrainment relation for the linearly stratified fluid was not different from the value in a two-layer fluid (see figure 4). Wave motions were, however, generated in the stably stratified layer adjacent to the interface, as shown for instance in figure 9(*a*), which is a streakline photograph taken in a situation where relatively strong wave activity was observed. To evaluate the importance of these waves in the mixing process is not a simple matter. Linden (1975) expressed the energy leakage rate by $L = \rho_0 a^2 N^3 \lambda / 3\pi\sqrt{3}$, where a and λ are the wave amplitude and wavelength, which he compared with the rate of potential-energy increase in the mixed layer. The expression for the ratio of the two is

$$A = \frac{4}{3\pi\sqrt{3}} \frac{a^2 \lambda N}{[(d^2 - d_0^2) + 2Rd_0^2]\dot{d}},$$

where $d = D + z_0$ and $R = g\Delta\rho_0/\rho_0 N^2 d_0$ and the dot represents the time derivative. The value of A depends on the choice of a and λ. Taking $a = h$ and $\lambda = \pi l$, we get for the conditions shown in figure 9(*a*) a value of $A = 0.3$. According to Linden's criteria, energy radiation by internal waves should not be negligible in this case.

A direct evaluation of the kinetic wave energy from figure 9(*a*) gives $(2u_w^2 + w_w^2)/3u^2 \simeq 0.020$ at $D + 3.8$ cm and 0.013 at $D + 11.5$ cm. The value of D in figure 9 is 26.6 cm and u has been evaluated at $z = D$. The wave-energy flux is

$$F_w \approx \rho q_w \frac{\lambda}{2\pi} N,$$

which should be compared with the energy flux into the interface. With $N = 1.25\ \mathrm{s}^{-1}$ and $\lambda = \pi l$ we find

$$\frac{F_w}{\frac{3}{2}\rho u^3} \approx \frac{(2u_w^2 + w_w^2)\, lN}{6u^3} = 0.03\dagger.$$

In the absence of an interface, with the turbulent layer adjacent to the fluid layer with a stratification of constant N, this ratio should be about 0.12 according to the theory of Carruthers & Hunt (1986); note that these authors compared E_w with u^3 rather than $\frac{3}{2}u^3$. Damping of the interfacial layer could explain this difference. For conditions corresponding to figure 9(*a*) the interface stratification $N_I \approx 3.7\ \mathrm{s}^{-1}$, giving $N_I l/u = 8.5$, which is close to conditions for maximum wave energy (Carruthers & Hunt). In the interface, wave motion is therefore likely to be predominant, but only a small amount of energy escapes into the constant-gradient layer.

Encouraged by the work of Carruthers & Hunt, we attempted to run an experiment with conditions close to their criterion for maximum wave-energy radiation. A uniform-density layer of 21 cm depth was placed above a constant-density-gradient layer with $N = 1.12\ \mathrm{s}^{-1}$. The grid was placed at $z_0 = 6$ cm below the free surface and was oscillated with a stroke of 2 cm and a frequency of 2 Hz. Initially the interface was located at $D_0 = 7.5$ cm and there was no interfacial layer between the homogeneous

† This ratio could be larger by a factor of up to two because of the potential-wave-energy part which was not included in q_w. The importance of wave reflection from the boundary is not known either. It can, however, be argued that because the measured value of q_w would contain the reflected wave energy and because the reflected wave-energy flux would have to be subtracted from q_w given above, the effect of wave reflection would be to decrease the value of the given energy ratio.

and the constant-gradient layers. A streak photograph showing the mixed-layer turbulence and the wave motion in the stably stratified layer is presented in figure 9(*b*). In this photograph $D \approx 17$ cm and $Nl/u = 5$. The particles in the stable layer have a free-fall velocity of about 0.5 cm s^{-1}. The ratio of kinetic wave energy $\frac{1}{2}\rho(2u_w^2 + w_w^2)$ to the incoming turbulent kinetic energy $\frac{3}{2}\rho u^2$ is about 0.015 at $D_0 + 10$ cm in this photograph. Since in this experiment l is smaller than in the conditions of figure 9(*a*), the ratio of wave-energy flux to turbulent kinetic-energy flux is even smaller than 0.03, meaning that wave-energy radiation remains unimportant.

The mixed-layer deepening rate was also measured. Initially there was a rapid deepening, as would be expected until a density interface built up. At long times (after about 30 min) when the mixed layer had deepened by about 3 cm, the deepening rate followed again the $t^{\frac{1}{2}}$ power law with a value of K_2 close to that given in table 1. It should be noted that this value of K_2 corresponds to a value of K in the entrainment relation (9) identical with that in the two-layered fluid.

A further experiment with $D_0 = 15$ cm, $z_0 = 6$ cm, $\Delta\rho_0/\rho_1 = 0.01$, $N = 0.24$ s^{-1} and $S = 2$ cm with $f = 5$ Hz, which comes closer to Linden's situation, also indicated no measurable effect of wave-energy radiation on the entrainment rate.

6. Conclusions

It has been shown that mixed-layer deepening in two-layer and linearly stratified fluid by turbulence generated with an oscillating grid obeys a power-law relation in time valid in the depth range where secondary effects remain negligible. These power laws are consistent with an entrainment relation $E = KRi^{-n}$ with $n = 1.5 \pm 0.05$, where $E = u_e/u$ and $Ri = g\Delta\rho l/\bar{\rho}u^2$ are defined with turbulence length and velocity scales near the interface, with the entrainment velocity calculated from the mixed-layer deepening rate $u_e = \mathrm{d}D/\mathrm{d}t$. This power-law exponent, valid when $Ri \gtrsim 7$ and when the Péclet number is large, differs from Fernando & Long's (1983) value but substantiates earlier findings by Turner (1968) and Hopfinger & Toly (1976) obtained under different conditions; the mixed-layer depth was kept constant in the latter two experiments, which eliminates any uncertainty concerning turbulence decay in the mixed layer. An explanation for the different results obtained by Fernando & Long may be found in the possible existence of relatively strong secondary motions generated by unsatisfactory near wall conditions of the grid. This is inferred from their large value of K in the entrainment relation.The lower limit of $Ri \approx 7$ corresponds to an interfacial Froude number $u/N_I l \approx 0.3$, which is close to the value of maximum internal wave generation (Carruthers & Hunt 1986).

The mechanisms of mixing that can explain an $Ri^{-\frac{1}{2}}$ power law have in common that the turbulent kinetic energy is made available for mixing at the buoyancy timescale rather than at the turbulence timescale l/u. Both direct recoil of an eddy and internal-wave breaking have the same timescale. The occurrence of one or the other event may depend on the angle of incidence of an incoming eddy.

The proportionality coefficient K has the same value ($K \approx 3.8$) in the two-layer and the constant-gradient fluids, which indicates that energy radiation by internal waves in the stratified layer adjacent to the interface is of no importance in the mixing process or mixing rate. The wave-energy flux in the stable layer is typically a few per cent (less than about 5% under most circumstances) of the turbulent kinetic energy flux into the interface. The interface acts as a filter for energy transfer to internal waves in the stable layer.

The interface thickness, defined by $h = (\mathrm{d}\rho/\mathrm{d}z)_{\max}/\Delta\rho$, normalized by the mixed-layer depth, has been shown to be a function of Richardson number in the form $h/D = 0.055 + 0.91\ Ri^{-1}$. This variation is similar to that observed in penetrative convection (Deardorff *et al.* 1980), though the numerical values differ mainly because of the different definition of the interface thickness used.

REFERENCES

Barla, K. 1980 Etude de l'entrainement turbulent à travers une interface de densité. Thèse de Docteur-Ingénieur, Université de Grenoble I.

Browand, F. K. & Hopfinger, E. J. 1985 The inhibition of vertical turbulent scale by stable stratification. *IMA Conf. Proc. Cambridge, 1983*. Clarendon.

Carruthers, D. J. & Hunt, J. C. R. 1986 Velocity fluctuations near an interface between a turbulent region and a stably stratified layer. *J. Fluid Mech.* **165**, 475.

Crapper, P. F. & Linden, P. F. 1974 The structure of turbulent density interfaces. *J. Fluid Mech.* **65**, 45.

Deardorff, J. W., Willis, G. E. & Stockton, B. H. 1980 Laboratory studies of the entrainment zone of a convective mixed layer. *J. Fluid Mech.* **100**, 41.

Dickey, T. D. & Mellor, G. L. 1980 Decaying turbulence in neutral and stratified fluids. *J. Fluid Mech.* **99**, 13.

Fernando, H. J. S. & Long, R. R. 1983 The growth of a grid-generated turbulent mixed layer in a two-fluid system. *J. Fluid Mech.* **133**, 377.

Fernando, H. J. S. & Long, R. R. 1985 On the nature of the entrainment interface of a two-layer fluid subjected to zero-mean-shear turbulence. *J. Fluid Mech.* **151**, 21.

Hopfinger, E. J. & Toly, J. A. 1976 Spatially decaying turbulence and its relation to mixing across density interfaces. *J. Fluid Mech.* **78**, 155.

Linden, P. F. 1973 The interaction of a vortex ring with a sharp density interface: a model for turbulent entrainment. *J. Fluid Mech.* **60**, 467.

Linden, P. F. 1975 The deepening of a mixed layer in a stratified fluid. *J. Fluid Mech.* **71**, 385.

Linden, P. F. 1979 Mixing in stratified fluids. *Geophys. Astrophys. Fluid Dyn.* **13**, 3.

Long, R. R. 1978 A theory of mixing in a stably stratified fluid. *J. Fluid Mech.* **84**, 113.

McDougall, T. J. 1979 Measurements of turbulence in a zero-mean-shear mixed layer. *J. Fluid Mech.* **94**, 409.

Mory, M. & Hopfinger, E. J. 1985 Rotating turbulence evolving freely from an initial quasi 2D state. *Macroscopic Modelling of Turbulent Flows*. Lecture Notes in Physics, vol. 230. Springer.

Rouse, H. & Dodu, J. 1955 Turbulent diffusion across a density discontinuity. *Houille Blanche* **10**, 522.

Thomson, S. M. & Turner, J. S. 1975 Mixing across an interface due to turbulence generated by an oscillating grid. *J. Fluid Mech.* **67**, 349.

Turner, J. S. 1968 The influence of molecular diffusivity on turbulent entrainment across a density interface. *J. Fluid Mech.* **33**, 639.

Turner, J. S. 1973 *Buoyancy Effects in Fluids*. Cambridge University Press.